

Analysis of Stress and Temperature Dependence of Fluorescence in $\text{SrTiO}_3:\text{Cr}^{3+}$

J. C. SLONCZEWSKI*

IBM Research Laboratory, 8803 Rueschlikon, Switzerland

(Received 27 April 1970)

We write a configurational potential for SrTiO_3 which depends on strain and the soft optic-mode coordinates whose wave vector lies at the corner of the Brillouin zone. Minimizing this potential gives the static response of the crystal to applied stress. Below the cubic-to-tetragonal transition temperature at 106°K , uniaxial stress applied in the $[111]$ direction induces a transition from the natural tetragonal to a trigonal phase, but transitions for $[100]$ and $[110]$ stresses are not found. A crystal-field calculation gives the R -line emission energy of Cr^{3+} impurities. The results fit the temperature-dependence anomaly found by Stokowsky and Schawlow and, within limits, the pressure dependence found by Burke and Pressley. However, pronounced discrepancies appear at stresses along the $[100]$ and $[110]$ directions which exceed critical values of 10 and 57 kg/mm^2 , respectively, suggesting that new phases of unknown character appear. The crystal-field parameter values inferred from the comparison with experiment support the nearest-neighbor approximation for the cubic component of the crystal-field, but not for lower-symmetry components. Our calculations disagree with a reported measurement of the stress dependence of the transition temperature.

I. INTRODUCTION

This work continues earlier calculations of properties of strontium titanate related to the structural transition at 106°K .¹ We refer the reader to the Introduction of the earlier paper (which we refer to as ST), and references given there, for a general orientation to the subject. In ST, we derived relations connecting spontaneous distortion, frequencies of zone-corner modes, and elastic constants of the tetragonal low-temperature phase. The available data were sufficient to determine the model parameters and to show some degree of consistency. Lauberau has made similar calculations, including also acoustic damping effects.²

Feder and Pytte have given a more fundamental theory of strontium titanate, based on statistical mechanics of anharmonic vibrations, which covers much of the same experimental ground.³ Their theory is an extension of their earlier work which had neglected strain effects,⁴ and is related to Pytte's calculation of ultrasonic attenuation.⁵ Our phenomenological Devonshire, or configurational potential, theory has been justified to some degree by lattice statistics.⁶ The question of its validity merits more attention, however, because of Pytte and Feder's finding^{3,4} that the lower soft-mode frequency is not exactly proportional to the square of the order parameter as predicted by the phenomenological theory employing only one temperature-dependent coefficient. We use the phenomenological theory, in spite of this and other¹ defects of principle, because of its success up to this date and because it is easily extended to include new effects.

In this work we analyze the dependence of chromium-impurity fluorescence on temperature^{7,8} and applied stress.⁹ In particular, Burke and Pressley's proposal of a transition to a trigonal phase induced by $[111]$ stress⁹ is confirmed quantitatively by our analysis. However, certain discrepancies, which can in no way be reconciled with the present theory, arise at critical $[100]$ and

$[110]$ stresses. Their natures suggest the existence of new stress-induced phases, but the characters of these phases are not established.

Section II is devoted to the form of the configurational potential. Section III describes the responses of the crystal to applied stresses for linear cases. Section IV presents a numerical computation of the nonlinear response and phase transition that occur under $[111]$ stress. Section V gives a crystal-field theory of chromium-impurity emission energies. Section VI describes the stress dependence of the emission lines. Section VII compares the theory with experiment. Section VIII discusses implications of the numerical values of the crystal-field parameters. An Appendix connects our work with recent studies of stress dependence of transition temperature.

II. ENERGY EXPRESSION

We extend our earlier work (ST) to include the effects of applied stresses. The configurational potential U (in units of energy per unit reference volume) depends on the soft-mode lattice coordinates $\mathbf{Q} = (Q_1, Q_2, Q_3)$, the strain coordinates e_{ij} or e_r defined by the equations

$$e_{ii} \equiv e_i \equiv \partial \xi_i / \partial x_i \quad (i=1, 2, 3), \quad (2.1)$$

$$e_{23} \equiv e_4 \equiv \partial \xi_2 / \partial x_3 + \partial \xi_3 / \partial x_2, \quad e_{31} \equiv e_5, \text{ etc.}, \quad (2.2)$$

where ξ_i and x_i are displacement and position coordinates, respectively, and the applied stress-tensor components $T_i \equiv T_{ii}$ ($i=1, 2, 3$), $T_4 \equiv T_{23}$, etc. The vector \mathbf{Q} describes linear oxygen displacements which correspond, in first order, to a simultaneous rotation of oxygen octahedra about titanium centers as described fully in ST. The Cartesian components Q_k ($k=1, 2, 3$) are normalized to be numerically equal to the oxygen displacements.

Symmetry arguments show easily that the leading

terms in a series expansion of U have the form

$$\begin{aligned}
 U = & U_0 + \frac{1}{2}KQ^2 + A'Q^4 + A_n(Q_1^2Q_2^2 + Q_2^2Q_3^2 + Q_3^2Q_1^2) \\
 & - B_e[(2e_1 - e_2 - e_3)Q_1^2 + (2e_2 - e_3 - e_1)Q_2^2 \\
 & + (2e_3 - e_1 - e_2)Q_3^2] - B_t(e_4Q_2Q_3 + e_5Q_3Q_1 + e_6Q_1Q_2) \\
 & + \frac{1}{2}C_{11}(e_1^2 + e_2^2 + e_3^2) + C_{12}(e_1e_2 + e_2e_3 + e_3e_1) \\
 & + \frac{1}{2}C_{44}(e_4^2 + e_5^2 + e_6^2) - \sum_i^6 e_i T_i. \quad (2.3)
 \end{aligned}$$

This expression without the last term is equivalent to Eqs. (1) and (2) of ST. As before we have simplified the energy expansion by omitting the coupling between \mathbf{Q} and the isotropic strain (A_1 representation) which would be embodied in a term proportional to $(e_1 + e_2 + e_3)Q^2$. The term $-\sum_i^6 e_i T_i$ in (2.3) represents the interaction with applied stress. Of all the parameters in this equation only U_0 and K are usually assumed to depend on entropy if U is internal energy, or on temperature if U is the Helmholtz free energy. In principle, we make the former choice to calculate correctly adiabatic elastic constants, although in application to SrTiO₃ we believe it makes little quantitative difference.¹ In any case, the condition $K < 0$ characterizes the noncubic phase and $K > 0$ the cubic phase.

The equilibrium configuration is found by minimizing U with respect to \mathbf{Q} and all e_i . It is convenient now, as in ST, to proceed half-way by varying e_i for arbitrary \mathbf{Q} . Letting $\partial U / \partial e_i = 0$, for all i , in (2.3), we find

$$e_i = C_e^{-1}[B_e(3Q_i^2 - Q^2) + T_i] - \delta \quad (i=1, 2, 3), \quad (2.4)$$

$$e_4 = (B_t Q_2 Q_3 + T_4) C_t^{-1}, \quad e_5 = \text{etc.}, \quad (2.5)$$

where our elastic constants are

$$C_e \equiv C_{11} - C_{12}, \quad C_t \equiv C_{44} \quad (2.6)$$

in the usual notation, and

$$\delta = C_{12}(T_1 + T_2 + T_3)(C_{11}^2 + C_{11}C_{12} - 2C_{12}^2)^{-1}. \quad (2.7)$$

Upon substitution of (2.4)–(2.7) into (2.3), one finds that U reduces to \tilde{U} , where

$$\begin{aligned}
 \tilde{U} = & \tilde{U}_0 \{ T_i \} + \frac{1}{2}KQ^2 + A'Q^4 + A_n'(Q_1^2Q_2^2 + Q_2^2Q_3^2 + Q_3^2Q_1^2) \\
 & - B_e C_e^{-1}[(2T_1 - T_2 - T_3)Q_1^2 + (2T_2 - T_3 - T_1)Q_2^2 \\
 & + (2T_3 - T_1 - T_2)Q_3^2] \\
 & - B_t C_t^{-1}(T_4 Q_2 Q_3 + T_5 Q_3 Q_1 + T_6 Q_1 Q_2). \quad (2.8)
 \end{aligned}$$

Here the form of the function \tilde{U}_0 is of no consequence since it does not depend on \mathbf{Q} . The subscripts e and t on B and C correspond to the irreducible representations E_g and T_{2g} of the cubic point group. The coefficients A' and A_n' are, as in ST, given by

$$A' = A - 3B_e^2 / C_e, \quad (2.9)$$

$$A_n' = A_n + 9B_e^2 / C_e - B_t^2 / 2C_t. \quad (2.10)$$

Finding the equilibrium values of \mathbf{Q} and e_i reduces to

minimizing \tilde{U} with respect to \mathbf{Q} , and then substituting the equilibrium \mathbf{Q} into (2.4) and (2.5).

The analysis by Pietrass and Hegenbarth¹⁰ of the stress dependence of the transition temperature, as measured by Sorge *et al.*,¹¹ is based on a configurational potential similar to our (2.8). They assumed an interaction term for the special case $Q_1 = Q_2 = 0$ equivalent to the expression

$$[b_1 T_3 + b_2 (T_1 + T_2)] Q_3^2$$

(with new coefficients b_1 and b_2) embracing both A_1 and E_g representations.

Neglecting the isotropic A_1 interaction is equivalent to setting b_2/b_1 ($=g_{12}/g_{11}$ in the notation of Ref. 10) equal to $-\frac{1}{2}$. This expression reduces to the corresponding term in (2.8) with $B_e = C_e b_2$. The analysis of SrTiO₃ data by Pietrass and Hegenbarth¹⁰ results in the value $g_{12}/g_{11} = -0.54$, which makes our neglect of the A_1 interaction appear reasonable. As pointed out in ST, the absence of a significant discontinuity in the thermal coefficient of expansion of SrTiO₃ at the transition temperature¹² also supports this simplifying assumption. Although we agree with Pietrass and Hegenbarth in this qualitative consideration, we disagree quantitatively with respect to the magnitude of the E_g interaction (see Appendix).

III. LINEAR DISTORTIONS

Here we carry out the minimization program insofar as we can by analytic means. Suppose a normal pressure p with direction cosines $\alpha_1, \alpha_2, \alpha_3$ is applied. Then the applied-stress tensor is

$$T_{ij} = -p\alpha_i\alpha_j. \quad (3.1)$$

Even with this substitution, (2.8) cannot be minimized in general by analytical means. However, there are special cases in which the unit vector $\mathbf{Q}Q^{-1}$ does not vary with p so that (2.8) reduces to the form

$$\tilde{U} = \tilde{U}_0 + \frac{1}{2}KQ^2 + aQ^4 + bpQ^2, \quad (3.2)$$

where a and b are constants, and an extremum is given by

$$Q^2 = -(4a)^{-1}(K + 2bp). \quad (3.3)$$

From this, together with (2.4) and (2.5), we see that e_i and the products $Q_i Q_j$ are linear in p for all i and j . As we shall see presently, the crystal-field matrix elements of the electronic Hamiltonian for the chromium impurity are linear forms in e_i and $Q_i Q_j$, so that these particular distortions are appropriately called linear.

The results for three linear cases relevant to Burke and Pressley's piezofluorescence experiments on strontium titanate⁹ are given below, together with remarks about stability, but proofs are omitted. The parameters C_e, C_t , and A' are positive for a stable crystal. We assume, also, that $-K, A_n'$, and B_e are positive, as we

know to be the case in SrTiO₃ below the transition temperature of 106°K, but the sign of B_i is not specified.

$$[100] \text{ case: } \mathbf{p} = p(1, 0, 0).$$

An equilibrium state is described by $\mathbf{Q} = Q(0, 0, \pm 1)$ or $Q(0, \pm 1, 0)$, together with the equation

$$Q = \left(\frac{-K - 2B_i p / C_i}{4A'} \right)^{1/2}. \quad (3.4)$$

Exhaustive analysis shows that this state is absolutely stable for all parameter values consistent with the algebraic signs assumed above. We interpret this result to mean that stress in the [100] direction cannot induce a phase transition in our model.

$$[110] \text{ case: } \mathbf{p} = (1/\sqrt{2})p(1, 1, 0).$$

One finds that the state $\mathbf{Q} = \pm Q(0, 0, 1)$ with Q given by (3.4) above provides equilibrium in this case, too. Although we failed to analyze this case exhaustively, we did find additional stable states with different orientations of \mathbf{Q} . We omit the details and merely remark that we did not succeed in finding states with lower energy than the one described for pressures in the range studied by Burke and Pressley and the parameter values used later in this report. Thus we have no reason to expect [110] stress to induce a transition in SrTiO₃ although we have no proof of its impossibility.

$$[111] \text{ case: } \mathbf{p} = (1/\sqrt{3})p(1, 1, 1).$$

A locally stable state is given by the equation

$$\mathbf{Q} = \pm \left(-\frac{K + 2B_i p / 3C_i}{12A' + 4A_n'} \right)^{1/2} \times (1, 1, 1) \quad (3.5)$$

under the conditions $p > p_L$ and $B_i < 0$, where

$$p_L = 3C_i A_n' K / B_i (9A' + A_n'). \quad (3.6)$$

When $p < p_L$, this state is unstable with respect to a rotation of \mathbf{Q} . Although we failed to find an analytic expression for the low-stress state in this case, we know that a phase transition must occur.

IV. STRESS-INDUCED TRANSITION

In the previous section we found by analytic means that application of stress along [100] and [110] directions in SrTiO₃ should produce linear distortions and we found no indication of changes that could be regarded as phase changes. In the case of a [111] stress, we found a locally stable linear response under the conditions that $B_i < 0$ and $p > p_L$. More complete analysis of the [111] case requires numerical computations, which we present here.

Taking again $\mathbf{p} = (1/\sqrt{3})p(1, 1, 1)$ we assume the equation

$$Q_2 = Q_1 \quad (4.1)$$

and that Q_3 may differ from Q_1 . It is plausible that such

a state is intermediate to the tetragonal state $\mathbf{Q} = (0, 0, Q)$ for $p = 0$ and the trigonal state

$$\mathbf{Q} = (1/\sqrt{3})Q(1, 1, 1),$$

which is locally stable for $p > p_L$. We neglect the possibility of a completely general orientation for \mathbf{Q} , although it cannot be logically excluded.

We eliminate Q_2 from (2.8) by means of (4.1), then set $\partial \tilde{U} / \partial Q_1 = \partial \tilde{U} / \partial Q_3 = 0$ to find the equations

$$0 = 3KQ_1 + 12A'(2Q_1^2 + Q_3^2)Q_1 + 6A_n'Q_1(Q_1^2 + Q_3^2) + B_i p(Q_1 + Q_3) / C_i, \quad (4.2)$$

$$0 = 3KQ_3 + 12A'(2Q_1^2 + Q_3^2)Q_3 + 12A_n'Q_3Q_1^2 + 2B_i p Q_1 / C_i. \quad (4.3)$$

Rather than solve this pair of cubics in Q_1 and Q_3 , we eliminate p between them to find the equation

$$4A'Q_3^4 + 4A'Q_1Q_3^3 + KQ_3^2 + (KQ_1 + 8A'Q_1^3 + 4A_n'Q_1^3)Q_3 - 2KQ_1^2 - 16A'Q_1^4 - 4A_n'Q_1^4 = 0. \quad (4.4)$$

It is convenient to assume a value for Q_1 , solve the quartic (4.4) for Q_3 numerically, and then find p from (4.3).

Generally, several solutions are found and one selects the one with lowest \tilde{U} , checking for local stability in three dimensions by investigating second-order differentials of \tilde{U} in the usual way. We present here results of numerical computations carried out on a remote computer terminal.

We choose parameter values which are appropriate to SrTiO₃ at 4.2°K. Thus, $M = 0.897 \text{ g/cm}^3$ is the mass of two oxygen atoms per chemical formula unit; $\rho = 5.13 \text{ g/cm}^3$; $C_e = C_{11} - C_{12} = 2.29 \times 10^{12}$, $C_a = C_{11} + 2C_{12} = 5.5 \times 10^{12}$, and $C_t = C_{44} = 1.27 \times 10^{12} \text{ erg/cm}^3$ are elastic constants of the cubic phase extrapolated to 4.2°K from empirical formulas of Bell and Rupprecht,¹³ neglecting $|T - T_c|^{-1}$ terms.

The five remaining parameters K , A , A_n , B_e , and B_i are derived, by inverting formulas of ST, from the following five quantities measured at 78°K: Raman frequencies $(2\pi)^{-1}\omega_1 = 3.5 \times 10^{11}$ and $(2\pi)^{-1}\omega_3 = 1.05 \times 10^{12} \text{ Hz}$,¹⁴ spontaneous oxygen displacement $Q_s = 5 \times 10^{-10} \text{ cm}$ [measured: $(4.7 \pm 1.2) \times 10^{-10} \text{ cm}$],¹⁵ $\Delta V_t = 3.9 \times 10^4 \text{ cm}^3/\text{sec}$, and $\sigma_s = 5.5 \times 10^{-4}$. The first three of these quantities are essentially experimental values obtained from the references quoted. The fourth, ΔV_t , is the step change in the [111]-longitudinal ultrasonic sound velocity at the transition temperature,¹³ as extracted from the published data by the present author [see Eqs. (29), (30), and (34) of ST]. The fifth, the spontaneous tetragonal strain σ_s , lies between the neutron backscattering value of Alefeld (4.0×10^{-4}),¹² and the x-ray value of Lytle (6.7×10^{-4}).¹⁶ Our choice of a numerical value for σ_s is a compromise between a fit of our theory to the critical stress to be discussed and to piezo-Raman measurements.¹⁷

The value of K (78°K) thus determined is adjusted to 4.2°K by direct proportionality (factor=1.94) to the rhombic splitting of the EPR spectrum of $\text{Fe}^{3+}-\text{V}_\text{O}^{-2}$ centers.^{1,18} The sign of B_i is not determined by the data presented. We choose $B_i < 0$ because this is the only possibility for a trigonal phase (Sec. III) and therefore for explaining Burke and Pressley's [111] data.⁹ Thus the parameter values are (in cgs units) K (4.2°K) = -3.08×10^{25} , $A = 1.95 \times 10^{43}$, $A_n = -2.41 \times 10^{42}$, $B_c = 1.68 \times 10^{27}$, and $B_t = -2.51 \times 10^{27}$. (We remark, however, that this set of values is not consistent with a recent report of stress dependence of the transition temperature, as discussed in the Appendix.) We note parenthetically that our value of A_n is negative, tending to favor trigonal distortion. This tendency is counteracted by the strain coupling which reverses the sign of the anisotropy ($A_n' = 6.19 \times 10^{42}$).

The results of our computation are illustrated in the $(1\bar{1}0)$ section of \mathbf{Q} space shown in Fig. 1. Initially, for $p=0$, \mathbf{Q} lies parallel to the [001] axis. With increasing stress p applied parallel to the [111] axis in the range $0 < p < p_c$, \mathbf{Q} progresses continuously in the $(1\bar{1}0)$ plane, with a slight (<1%) decrease in magnitude as shown by the solid curve. This curve represents an intermediate phase which is neither tetragonal nor trigonal. At a critical value $p=p_c=23.0$ kg/mm², a first-order transition occurs and the perfectly trigonal state $\mathbf{Q} = (1/\sqrt{3})\mathbf{Q}(1, 1, 1)$ becomes stable. Further increases in p cause \mathbf{Q} to increase in magnitude without deviating from the [111] axis, as shown by the solid line.

From (3.6) one finds that the trigonal phase is locally stable down to 19.8 kg/mm², at a \mathbf{Q} value 0.1% smaller than that for $p=p_c$. Also, numerical analysis shows that the pseudotetragonal phase is stable a fraction of 1 kg/mm² above p_c . Thus, in principle,

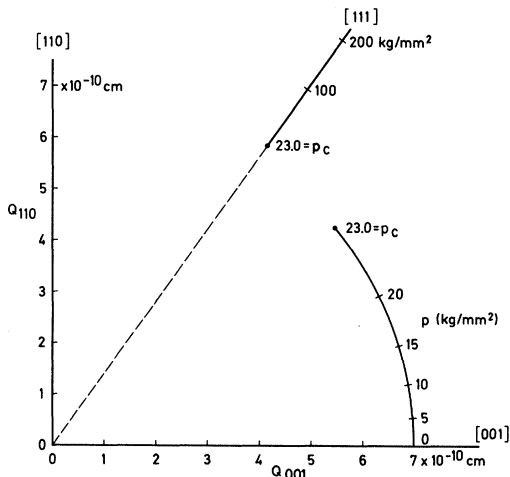


FIG. 1. $(1\bar{1}0)$ section of soft-mode-coordinate space. The curve is a locus of calculated stable points \mathbf{Q} as a function of stress p applied parallel to the [111] axis at $T=4.2^\circ\text{K}$. The critical stress $p_c=23.0$ kg/mm² separates trigonal and pseudotetragonal phases.

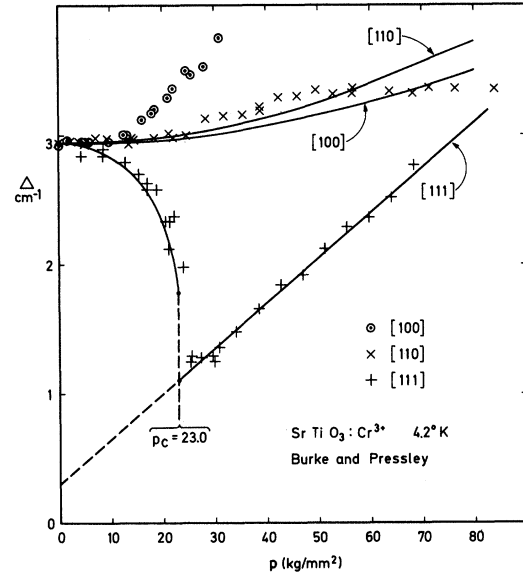


FIG. 2. Splitting Δ of R lines in $\text{SrTiO}_3:\text{Cr}^{3+}$ versus stress p applied parallel to principal axes. Curves calculated with four adjusted parameters.

cycling of p could give rise to hysteresis involving metastable states of either kind. Indeed the energy differences are slight [$<1\%$ of $|U(0) - U(p_c)|$], suggesting that something of this kind could happen. Since small adjustments to the theory or small experimental disturbances could overwhelm this small difference, it may be well to consider the critical stress as being undetermined by this amount (~ 3 kg/mm²).

In summary, parameter values consistent with independent experimental data for SrTiO_3 give rise to a nonlinear behavior and a distinct phase transition when stress is exerted along the [111] axis. The predicted transition stress at 4.2°K is in the range 20–23 kg/mm² as compared to the critical stress of 24–25.4 kg/mm² apparent in the chromium-fluorescence data of Burke and Pressley⁹ (see data points along curve [111] of our Fig. 2). Theory permits no transition in SrTiO_3 for stresses parallel to [100] directions, and we have not found any for [110] directions, as explained in Sec. III.

V. EMISSION ENERGIES

The initial states of the R doublet of Cr^{3+} in octahedral coordination belong to the excited $(3d\epsilon)^3 {}^3E$ level, and the final states belong to the ground $(3d\epsilon)^3 {}^4A_2$ level. Shawlow *et al.* pointed out, in their work on piezofluorescence of $\text{MgO}:\text{Cr}^{3+}$, that the splitting of the ground level by noncubic crystal fields should be negligible because it is an orbital singlet.¹⁹ This assumption is justified by Müller's EPR observation of 4.0×10^{-4} cm⁻¹ for the D parameter in the spin Hamiltonian for $\text{SrTiO}_3:\text{Cr}^{3+}$ at 80°K.²⁰ From this value and the temperature dependence of the tetragonal crystal field

discussed in ST one infers that the spontaneous splitting of 4A_2 is less than $2.0 \times 10^{-3} \text{ cm}^{-1}$ at all temperatures, or in the order of 10^{-3} as large as the observed R -line splitting (see Fig. 2).

We let ξ represent the set of configurational variables $\{e_i, Q_j\}$ and define an effective electronic Hamiltonian $V'(\xi)$ with the equations

$$H = H_0 + V(\xi),$$

$$V'(\xi) = V(\xi) - \langle {}^4A_2 | V(\xi) | {}^4A_2 \rangle. \quad (5.1)$$

Here H_0 is the electronic Hamiltonian which includes the cubic-field energy for $\xi=0$, and whose eigenstates include $|{}^2E\rangle$ and $|{}^4A_2\rangle$; $V(\xi)$ is the crystal-field energy due to the lattice distortion, with $V(0)=0$. Since we have subtracted the degenerate ground-level perturbation $\langle {}^4A_2 | V(\xi) | {}^4A_2 \rangle$ in the definition of V' , diagonalization of V' in the initial-state manifold yields the first-order change of emitted photon energy directly.

Since we are not especially concerned here with details of electron structure, we derive the matrix representation of V' from symmetry properties of the excited-state wave functions. By selecting a basis for the double-group representation Γ_8 of the cubic point group O (in the notation of Koster *et al.*²¹) which corresponds to 2E , we take formal account of spin-orbit effects. Spin-orbit coupling is important because it mixes the 2E with other Γ_8 states, some of which lie close in energy according to calculations.²²

Since the antisymmetric product $\{\Gamma_8^2\}$ equals $A_1 + E + T_2$, crystal-field components transforming according to these representations will interact with the Γ_8 level.²³ To derive the matrix of this interaction we follow a procedure partly suggested by Kane's theory of silicon valence bands.²⁴ We consider first a six-dimensional basis $u_i s_j$ consisting of products of the real orbital states u_1, u_2, u_3 , which transform according to the single-valued representation $T_1 (= \Gamma_4)$, and the spin states $s_1 = \downarrow$, $s_2 = \uparrow$. The "effective- p " states u_1, u_2, u_3 are assumed to transform among themselves under proper rotations just like the corresponding Cartesian coordinates X_1, X_2, X_3 (referred to the pseudocubic axes of the crystal). Spin quantization is assumed parallel to the X_3 axis. Since the spin states belong to Γ_6 , the product manifold $(\Gamma_4 \times \Gamma_6 = \Gamma_6 + \Gamma_8)$ ²¹ contains the twofold Γ_6 as well as the fourfold Γ_8 representation of interest.

Let us define \mathcal{K} to be the time-reversal operator²⁵

$$\mathcal{K} = \mathcal{C}\kappa, \quad (5.2)$$

where \mathcal{C} means complex conjugate, and κ is a spin operator with the properties

$$\kappa \uparrow = \downarrow, \quad \kappa \downarrow = -\uparrow. \quad (5.3)$$

Also let $\beta = \exp(\pi i/6)$, and consider the four linear

combinations of $u_i s_j$ defined by the equations

$$\begin{aligned} |1\rangle &= (1/\sqrt{3})(\beta^4 u_1 \downarrow + \beta^{-1} u_2 \downarrow + u_3 \uparrow), \\ |2\rangle &= (1/\sqrt{3})(\beta^4 u_1 \uparrow + \beta^5 u_2 \uparrow - u_3 \downarrow), \\ \mathcal{K}|1\rangle &= (1/\sqrt{3})(\beta^2 u_1 \uparrow + \beta^{-5} u_2 \uparrow + u_3 \downarrow), \\ \mathcal{K}|2\rangle &= (1/\sqrt{3})(\beta^{-4} u_1 \downarrow + \beta^{-5} u_2 \downarrow + u_3 \uparrow). \end{aligned} \quad (5.4)$$

An orthonormal basis, such as this one, in which half the vectors are Kramers conjugates of the other half is known as a Kramers basis. One can verify that the vectors (5.4) form a basis for Γ_8 . To show this, let \mathbf{L} be the pseudo-orbital-momentum operator which operates according to equations of the form

$$L_1 u_1 = 0, \quad L_1 u_2 = i u_3, \quad L_1 u_3 = -i u_2,$$

and others obtained by cyclic permutations of the indices. Also let $\boldsymbol{\sigma}$ be the Pauli spin operator. One can verify directly that the state vectors (5.4) have the eigenvalue $\frac{1}{4}$ for the operator $\mathbf{J} \cdot \mathbf{J} = (\mathbf{L} + \frac{1}{2}\boldsymbol{\sigma})^2$, or equivalently, the eigenvalue 1 for the operator

$$\mathbf{L} \cdot \boldsymbol{\sigma} = \frac{1}{2}(L_1 + iL_2)\sigma_- + \frac{1}{2}(L_1 - iL_2)\sigma_+ + L_3\sigma_3. \quad (5.5)$$

This set has total pseudomomentum $J = \frac{3}{2}$ and is known to transform according to Γ_8 .

The particular linear combinations (5.4) were chosen *a posteriori* to yield a simple expression for the matrix representation of V' to be derived. Using the fact that V' is real and spin independent one can show that its representation in a Kramers basis has the form²⁴

$$V'(\xi) = \begin{bmatrix} \mathbf{G} & \boldsymbol{\Lambda} \\ -\boldsymbol{\Lambda}^* & \mathbf{G}^* \end{bmatrix}, \quad (5.6)$$

where \mathbf{G} is a Hermitian submatrix with $G_{ij} = \langle i | V' | j \rangle$ and $\boldsymbol{\Lambda}$ is an antisymmetric submatrix with $\Lambda_{ij} = \langle i | V' \mathcal{K} | j \rangle$. The asterisk means complex conjugate.

We adopt the notation

$$M_{ii}(\xi) = 3^{-1} \langle u_i | V'(\xi) | u_i \rangle, \quad (5.7)$$

$$M_{i \neq j}(\xi) = - (1/\sqrt{3}) \langle u_i | V'(\xi) | u_j \rangle. \quad (5.8)$$

Using the fact that V' commutes with $\boldsymbol{\sigma}$, one finds by direct calculation from (5.4) the formulas

$$\mathbf{G} = \sum_j M_{jj} \begin{pmatrix} 1 & 0 \\ 0 & 1 \end{pmatrix} + \begin{pmatrix} M_{12} & M_{23} - iM_{13} \\ M_{23} + iM_{13} & -M_{12} \end{pmatrix}, \quad (5.9)$$

$$\boldsymbol{\Lambda} = (\gamma M_{11} + \gamma^* M_{22} + M_{33}) \begin{pmatrix} 0 & 1 \\ -1 & 0 \end{pmatrix}, \quad (5.10)$$

where $\gamma = e^{2\pi i/3}$. From the symmetry properties of M_{ij} one can verify that all of the representations contained in the antisymmetric product $\{\Gamma_8^2\} = A_1 + E + T_2$ ²³

contribute to our matrix for \mathbf{V}' . Thus we know that our Eqs. (5.6), (5.9), and (5.10), with (5.7) and (5.8) used only to determine the symmetry properties of M_{ij} , are general, even though the manifold (5.4) inaccurately represents the true wave functions.

In this system with an odd number of electrons and no applied magnetic field, the twofold Kramers degeneracy is not lifted. The 4×4 matrix \mathbf{V}' thus has two unequal eigenvalues ϵ_1 and ϵ_2 . We use the Schawlow *et al.* notations¹⁹ for mean line shift λ and splitting Δ given by

$$2\lambda = \epsilon_1 + \epsilon_2, \quad \Delta = |\epsilon_1 - \epsilon_2|. \quad (5.11)$$

The shift is simply

$$\lambda = 4^{-1} \text{Tr} \mathbf{V}' = \sum_j M_{jj}. \quad (5.12)$$

The splitting is found, by expanding the secular determinant of $\mathbf{V}' - \lambda$, to be

$$\Delta = 2 \left(\sum_{i \leq j} M_{ij}^2 - \sum_{i < j} M_{ii} M_{jj} \right)^{1/2}. \quad (5.13)$$

The symmetry properties described by the subscripts of M_{ij} , together with (5.12) and (5.13), express the dependence of the emission lines on an arbitrary perturbation of the original cubic crystal field.

VI. EQUATIONS FOR PIEZOFLUORESCENCE

To complete the theory we need to relate the matrix element M_{ij} to the distortion described by $\xi = \{Q_i, e_{ij}\}$. The formal results of the integrations indicated in (5.7) and (5.8) can be obtained by symmetry arguments. We recall that e_{ij} is a symmetric tensor and that \mathbf{Q} represents, in first order, a rotation of the oxygen octahedron surrounding a Cr^{3+} impurity. The components Q_i transform according to T_1 , which is not among the representations ($A_1 + E + T_2$) subtended by the set $\{M_{ij}\}$.

However, the set $\{Q_i Q_j\}$ of products and also the set $\{e_{ij}\}$ have precisely the same transformation properties as $\{M_{ij}\}$ with respect to cubic symmetry operations. Therefore we propose to approximate M_{ij} with linear functions of e_{kl} and $Q_k Q_l$ (all k, l).

First consider the shift λ , which is proportional to the change in cubic field. We approximate it with the lowest-order cubic invariant

$$\lambda = V_a Q^2 + W_a \sum_i e_{ii} \quad (6.1)$$

in which the constants V_a and W_a remain to be determined. Making use of (2.4) and (2.7), we eliminate e_{ii} to find

$$\lambda = V_a Q^2 + W_a (C_{11} + 2C_{12})^{-1} \sum_i T_{ii}. \quad (6.2)$$

To find the splitting Δ we note that considerations of symmetry dictate first-order relations of the form

$$M_{ii} = V_e Q_i^2 + W_e e_{ii} - f(Q^2, \sum_j e_{jj}) \quad (6.3)$$

and

$$M_{i \neq j} = V_t Q_i Q_j + W_t e_{ij}, \quad (6.4)$$

where the constants V_e , W_e , V_t , and W_t remain to be determined. Since f does not depend on i , Δ as given by (5.13) is independent of f . Therefore, we shall not write explicitly any additive term common to all M_{ii} ($i=1, 2, 3$) in the following discussion. Substituting (2.4) and (2.5) into (6.3) and (6.4), respectively, we find the relations

$$M_{ii} = U_e Q_i^2 + W_e (C_{11} - C_{12})^{-1} T_{ii} \quad (6.5)$$

with

$$U_e = V_e + 3W_e B_e (C_{11} - C_{12})^{-1} \quad (6.6)$$

and

$$M_{i \neq j} = U_t Q_i Q_j + W_t C_{44}^{-1} T_{ij} \quad (6.7)$$

with

$$U_t = V_t + W_t B_t C_{44}^{-1}. \quad (6.8)$$

Supposing $Q_i(\mathbf{T})$ to be known from the results of Secs. III and IV, $\lambda(\mathbf{T})$ is given by (6.2) and $\Delta(\mathbf{T})$ is given by (5.13), (6.5), and (6.7), and thus the variation of emission energy with applied stress is known. The terms $U_e Q_i^2$ and $U_t Q_i Q_j$ ($i=j$) in (6.5) and (6.7) combine the direct crystal field due to \mathbf{Q} with the indirect contribution through e_{ij} arising from internal stresses associated with coupling to \mathbf{Q} . Only the direct coupling term $V_a Q^2$ is present in (6.2) because we neglected coupling of Q to volume strain in (2.3). The remaining terms (linear in T_{ij}) of (6.2), (6.5), and (6.7) represent the crystal-field distortion due to stress in a linear medium, as in the work of Schawlow *et al.* on $\text{MgO}:\text{Cr}^{3+}$.

The results for the linear distortions considered in Sec. III are given below, with the subscripts on λ and Δ specifying the direction of p .

Shifts:

$$\lambda_{100} = \lambda_{110} = \frac{-KV_a}{4A'} + \left(\frac{V_a B_e}{2C_e A'} - \frac{W_a}{C_{11} + 2C_{12}} \right) p, \quad (6.9)$$

$$\lambda_{111} = \frac{-3KV_a}{12A' + 4A_n'} - \left(\frac{V_a B_t}{C_t (6A' + 2A_n')} + \frac{W_a}{C_{11} + 2C_{12}} \right) p. \quad (6.10)$$

Splittings:

$$\Delta_{100}^2 = \left(\frac{KU_e}{2A'} \right)^2 - \frac{KU_e}{A'C_e} \left(\frac{B_e U_e}{A'} + W_e \right) p + \left[\left(\frac{B_e U_e}{A'} \right)^2 + \frac{2W_e B_e U_e}{A'} + 4W_e^2 \right] \frac{p^2}{C_e^2}, \quad (6.11)$$

$$\Delta_{110}^2 = \left(\frac{KU_e}{2A'} \right)^2 - \frac{KU_e}{A'C_e} \left(\frac{U_e B_e}{A'} + W_e \right) p + [(U_e B_e A'^{-1} + W_e)^2 C_e^{-2} + W_t^2 C_t^{-2}] p^2, \quad (6.12)$$

$$\Delta_{111} = \left| \frac{-\sqrt{3}KU_t}{6A' + 2A_n'} - \frac{2}{\sqrt{3}C_t} \left(\frac{U_t B_t}{6A' + 2A_n'} + W_t \right) p \right|. \quad (6.13)$$

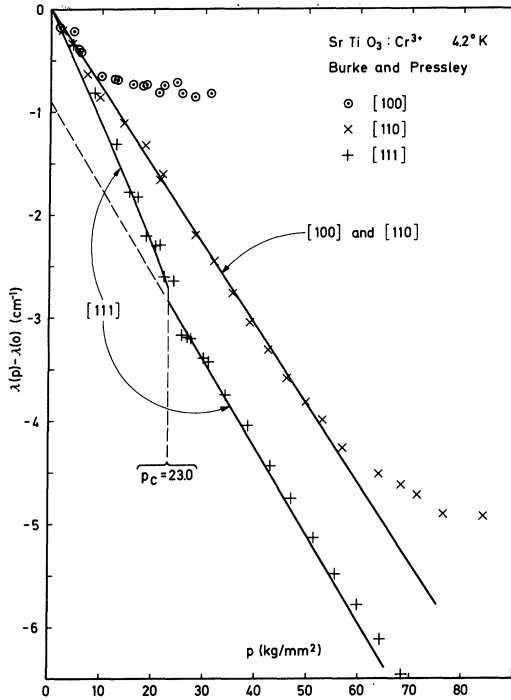


FIG. 3. Relative shift λ of mean R line in $\text{SrTiO}_3:\text{Cr}^{3+}$ versus stress p applied parallel to principal axes. Curves calculated with one adjusted parameter.

Here it should be remembered that (6.10) and (6.13) are subject to the condition $p > p_L$ with p_L given by (3.6), which describes local stability of the trigonal phase. We note that even when the crystal distortion as measured by $Q_i Q_j$ and e_{kl} is linear in p , in two cases (Δ_{100} and Δ_{110}) the emission energy is not linear because the matrix eigenvalues are not linear in M_{ij} .

In the nonlinear case of [111] stress with $Q_1 = Q_2 \neq Q_3$, we compute Q_3 and p as functions of Q_1 numerically, as described in Sec. IV. These values are substituted into the equation

$$\lambda_{111} = V_a Q^2 - W_a (C_{11} + 2C_{12})^{-1} p, \quad (6.14)$$

which follows from (6.2), and the equation

$$\Delta_{111}^2 = 4[(U_t Q_1^2 - W_t p / 3C_t)^2 + 2(U_t Q_1 Q_3 - W_t p / 3C_t)^2 + U_e^2 (Q_3^2 - Q_1^2)^2], \quad (6.15)$$

obtained from (5.13), (6.5), and (6.7).

VII. COMPARISON WITH EXPERIMENT

Before launching into a numerical comparison of the shifts (λ) and splittings (Δ) calculated in Sec. VI with the piezofluorescence experiments of Burke and Pressley,⁹ it is helpful to make some qualitative observations. First we note that λ_{100} and λ_{110} are exactly equal and linear in p , according to (6.9). The data for λ , shown in Fig. 3, are compatible with these predictions only up to

10 kg/mm² in the case of λ_{100} and up to 57 kg/mm² in the case of λ_{110} . At stresses exceeding these values, λ_{100} and λ_{110} make positive deviations from a common line. Second, according to our discussion in Sec. IV, [111] stress increasing from zero causes a transitional nonlinear behavior and, for $p > p_L$, linear dependences of λ_{111} and Δ_{111} given in (6.10) and (6.13). These features are consistent with the data in Figs. 2 and 3.

In view of these facts we will restrict quantitative comparisons to the regions $p < 10$ and $p < 57$ kg/mm² for [100] and [110] stresses, respectively. We provisionally ascribe the anomalies at higher stresses to the appearance of new phases. The entire experimental range of p will be considered in the [111] case.

Our computations require values for the six crystal-field coefficients $V_a, W_a, U_e, W_e, U_t, W_t$ which appear in (6.9)–(6.13). [We recall that V_i (or U_i) and W_i refer to optic-mode and strain coupling, respectively, while the subscripts $a, e,$ and t refer to the representations $A_1, E,$ and T_2 , respectively.] The remaining model parameters were already determined in Sec. IV.

Shifts

The only crystal-field parameters which influence the shifts are V_a and W_a . We estimate V_a from the temperature dependence of the R -line shift λ' in the absence of applied stress, observed by Stokowski and Shawlow and exhibited in Fig. 4 ($\lambda' = \Delta\nu$ in their notation).⁸ In the cubic phase above the transition temperature $T_c = 106^\circ\text{K}$, λ' varies with temperature because of (1) thermal expansion and (2) thermal dependence of vibronic interactions, as discussed by Stokowski and Shawlow.⁸ But our λ takes into account only effects of the static distortion which comes into play for temperatures $T < T_c$. Assuming these effects are additive, the discontinuous change in $d\lambda'/dT$ at $T = T_c$ may be attributed to our $d\lambda/dT$ ($p = 0$). Extrapolating

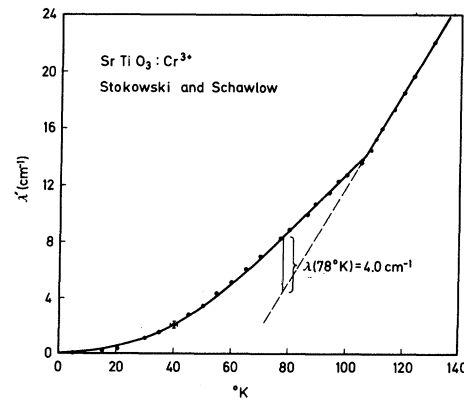


FIG. 4. Shift λ' of mean R line versus absolute temperature, in $\text{SrTiO}_3:\text{Cr}^{3+}$, for vanishing applied stress. Graphical determination of the parameter $\lambda(78^\circ\text{K}) = 4.0 \text{ cm}^{-1}$, used in calculating the curves in Fig. 3, is indicated.

TABLE I. Crystal-field parameters for SrTiO₃:Cr³⁺ and MgO:Cr³⁺.

<i>i</i>	SrTiO ₃				MgO
	<i>W_i</i> (cm ⁻¹)	<i>U_i</i> (cm ⁻¹ Å ⁻²)	<i>V_i</i> (cm ⁻¹ Å ⁻²)	<i>χ_i</i> (cm ⁻¹ Å ⁻²)	<i>W_i</i> (cm ⁻¹)
<i>a</i>	6400	1600 ^a	1600	-80	1300
<i>e</i>	-320	300 ^b	370	330	±660
<i>t</i>	-380	57 ^b	-19	-120	±360

^a By assumption $U_a = V_a$.^b By assumption $U_e > 0$ and $U_t > 0$.

the high-temperature curve down to $T=78^\circ\text{K}$ as indicated in Fig. 4, and subtracting the ordinate from λ' (78°K), we find $\lambda(p=0, T=78^\circ\text{K})=4.0\text{ cm}^{-1}$. Substituting this and our assumed $Q_s=5\times 10^{-10}\text{ cm}$ into the equation $V_a=\lambda Q_s^{-2}$, we find $V_a=1.6\times 10^{19}\text{ cm}^{-3}$.

Then we equate the coefficient of p in (6.9) to the experimental slope of λ_{110} to find $W_a=6.4\times 10^3\text{ cm}^{-1}$. Without further adjustment of parameters we calculate the curve $\lambda_{111}(p)-\lambda(0)$ which agrees substantially with the data, as shown in Fig. 3.

Splittings

According to (6.11) or (6.12), the splitting at vanishing stress is given by

$$\Delta(p=0) = |KU_e/2A'|. \quad (7.1)$$

The fact that the experimental⁷ splitting for zero stress varies with temperature in proportion to K , as predicted by (6.9), was noted in ST.

Computation of Δ as a function of p requires four parameters. The signs of U_e and U_t may be chosen arbitrarily because simultaneous reversal of U_e and W_e , or of U_t and W_t , does not change Δ . We let U_e and U_t be positive. Fitting these parameters to the data in Fig. 2, with emphasis on Δ_{111} , we find the values for U_e, W_e, U_t, W_t shown in Table I.

We find that the calculated curve for Δ_{111} in the transitional region agrees well with the data. The agreement for Δ_{100} and Δ_{110} is limited to lower stresses, with marked deviations for stresses above 10 kg/mm^2 in the case of Δ_{100} , and 57 kg/mm^2 in the case of Δ_{110} . These are the same critical stresses at which λ_{100} and λ_{110} , respectively, begin to deviate from theory.

VIII. DISCUSSION

Our account of the emission spectrum in SrTiO₃:Cr³⁺ is based on the same configurational potential and essentially the same parameter values with which ST accounted for certain independent data. We find good agreement with the emission data except for pronounced discrepancies which appear when the pressure exceeds critical values in the [100] and [110] directions. In particular, we confirm Burke and Pressley's proposal of a transition to a trigonal phase to explain the "anomalous" [111] data.^{9,26} This phase has the same trigonal pseudoperovskite structure possessed by the

compounds NdAlO₃, PrAlO₃, and LaAlO₃ in the absence of applied stress.²⁷ Indeed, the sign of the trigonal strain is the same, i.e., the sign of B_i (<0) we were required to choose in Sec. IV in order to explain the transition is the same as would be required to account, in these aluminates, for their spontaneous contraction along the trigonal axis relative to orthogonal directions.²⁸

In independent work, Rehwald²⁹ recently gave an account of the stress-induced transition to the trigonal phase. His configurational potential is precisely equivalent to ours. The principal difference in the analysis is that he neglects the departure of \mathbf{Q} from the [001] axis in the low-stress region. We find, however, that Q_{110} attains large values in the low-stress phase before the transition sets in (see Fig. 1).

Since the [100] and [110] anomalies are associated with apparently critical stresses, one is inclined to account for them also by phase transitions. The new phases might well be ferroelectric³⁰ because the ferroelectric mode is already quite soft at 4.2°K in the absence of applied stress, as indicated by a variety of measurements, including dielectric constant,³¹ Raman scattering with applied electric fields,^{14,32} chromium fluorescence with applied electric fields,³³ and EPR in electric fields.³⁴ Theoretical investigation of this possibility would require additional terms in the configurational potential and is beyond the scope of this paper.

We turn our attention now to implications of our crystal-field parameter values. In qualitative terms, the crystal-field coefficients $U_i, V_i,$ and W_i ($i=a, e, t$) as defined in Sec. VI have the following meanings: W_i measures the crystal field due to strain \mathbf{e} alone; V_i measures the crystal field due to optic-mode displacement \mathbf{Q} alone; U_i is the sum of V_i and an indirect strain contribution through internal stress caused by interaction of \mathbf{Q} and \mathbf{e} . The subscripts a, e, t identify the irreducible representations involved.

We now refer to the numerical values for SrTiO₃ shown in Table I. (We have $U_a=V_a$ by virtue of our neglect of the $Q-e$ interaction for this symmetry.) The fact that U_e and V_e are nearly equal, but U_t and V_t are not, indicates that in the former case the indirect contribution is small, whereas in the latter it is greater than the direct effect of \mathbf{Q} .

Since \mathbf{Q} and \mathbf{e} are mathematically independent

variables, we can test, in this system, the plausible assumption that the crystal field acting on a given impurity is determined principally by the positions of the nearest-neighbor ligands. Consider a pure rotation of a perfectly regular octahedron. It is true that, in first-order, \mathbf{Q} represents a rotation through an angle with components $2a^{-1}Q_i$, where a is the lattice parameter. In second order, strains may be combined with the linear displacement \mathbf{Q} in order to preserve the octahedral form, although of course more distant ions will execute nonrotational displacements. One finds the required strain components to be

$$e_{ii} = 2a^{-2}(Q_i^2 - Q^2) \quad (8.1)$$

and

$$e_{i \neq j} = 4a^{-2}Q_i Q_j. \quad (8.2)$$

Substituting these values into (6.1), (6.3), and (6.4) one finds the equations

$$\lambda = \chi_a Q^2 \quad \text{with} \quad \chi_a = V_a - 4a^{-2}W_a, \quad (8.3)$$

$$M_{ii} = \chi_e Q_i^2 - f \quad \text{with} \quad \chi_e = V_e + 2a^{-2}W_e, \quad (8.4)$$

$$M_{i \neq j} = \chi_t Q_i Q_j \quad \text{with} \quad \chi_t = V_t + 4a^{-2}W_t. \quad (8.5)$$

The constants χ_a , χ_e , and χ_t represent the crystal-field coefficients for displacements which only rotate each octahedron about its center. Numerical values for SrTiO_3 ($a = 3.9 \text{ \AA}$) are given in Table I.

In the case of strontium titanate, $|\chi_a|$ is quite small ($\chi_a/V_a = -0.05$); therefore the A component of the crystal field is predominantly caused by nearest neighbors. However, both $|\chi_e|$ and $|\chi_t|$ are quite large ($\chi_e/V_e = 0.90$, $\chi_t/V_t = 6.3$), showing that more distant ionic displacements do contribute appreciably to the E and T components of the crystal field.

We note that the leading term for a potential in a sourceless region of A_{1g} symmetry is a fourth-degree spherical harmonic, rather than second degree as in the case of E_g and T_{2g} . Thus the magnitudes of χ_i accord with the principle that lattice sums converge more rapidly for higher-order multipoles. This concrete evidence of long-range E_g and T_{2g} crystal-field contributions has important consequences for ligand-field³⁵ and local Jahn-Teller³⁶ theories, which are often based on nearest-neighbor assumptions. The Jahn-Teller coupling parameter found in EPR experiments on $\text{SrTiO}_3:\text{Ni}^{3+}$ could not be reconciled with its value in $\text{Al}_2\text{O}_3:\text{Ni}^{3+}$ on a local-strain basis.³⁷

It is worth remarking that in the absence of spin-orbit coupling the splitting of an E_g level by a crystal field of T_{2g} symmetry should vanish exactly. The fact that the coefficients relating to T_{2g} symmetry are not consistently smaller than the other indicates that the 2E_g level of Cr^{3+} is close to other Γ_8 levels, in qualitative accord with the level diagram calculated by Tanabe and Sugano.²²

We may relate our crystal-field coefficients to piezofluorescence studies in $\text{MgO}:\text{Cr}^{3+}$ by Schawlow *et al.*¹⁹

Since in this case there is no structural transition we set $A' = \infty$ in our equations (6.9)–(6.13). The shift for any direction of applied pressure is

$$\lambda = -W_a(C_{11} + 2C_{12})^{-1}p. \quad (8.6)$$

The splittings become, from (6.11)–(6.13),

$$\Delta_{100} = |2W_e C_e^{-1}|p, \quad (8.7)$$

$$\Delta_{111} = |(2/\sqrt{3})W_t C_t^{-1}|p, \quad (8.8)$$

and

$$4\Delta_{110}^2 = \Delta_{100}^2 + 3\Delta_{111}^2. \quad (8.9)$$

The point-charge crystal-field calculations of Schawlow *et al.* satisfy the relation (8.9). Substitution of their data makes the right-hand side of (8.9) exceed the left by 20%, which is a little more than the stated experimental error. Substituting their data into (8.6)–(8.8), we find the $|W_i|$ -values of the last column in Table I.³⁸ Although they are comparable in order of magnitude to the corresponding SrTiO_3 parameters they do not agree quantitatively. From our arguments given about the range of the crystalline-field interaction we would expect W_a to agree better than W_e and W_t , whereas the reverse may be true if the algebraic signs of W_e and U_t are consistent.

ACKNOWLEDGMENTS

The author is indebted to W. J. Burke and R. J. Pressley, and to W. Rehwald, for access to their works before publication, to Dr. Burke for helpful discussions, and to K. A. Müller for a critical reading of the manuscript.

APPENDIX

In a recent paper Pietrass and Hegenbarth¹⁰ have discussed the tension dependence of T_c in strontium titanate, as measured by Sorge *et al.*¹¹ They point out that tension τ_3 applied along the $[001]$ axis makes the state $\mathbf{Q} = (0, 0, Q)$ stable because of the sign of the strain interaction (our $B_e > 0$). In our notation, the configurational energy (2.8) becomes

$$\tilde{U} = [\frac{1}{2}K(T) - 2B_e C_e^{-1} \tau_3]Q^2 + A'Q^4. \quad (A1)$$

The transition temperature $T = T_c$ is found by setting the coefficient of Q^2 equal to zero. Differentiating this coefficient with respect to temperature we find for the tension dependence of T_c

$$\frac{dT_c}{d\tau_3} = \frac{4B_e}{C_e[dK(T_c)/dT]}. \quad (A2)$$

This is equivalent to the result of Pietrass and Hegenbarth if we assume the relation $g_{12}/g_{11} = -\frac{1}{2}$ in their equations, which is close to the value -0.54 that they find from the data.

According to soft-mode theory we have

$$K(T) = 4\pi^2 M v^2(T), \quad T > T_c \quad (A3)$$

where M is the mass density of the soft corner mode

and ν is its frequency for $T > T_c$; and

$$3B_e Q_s^2 = \sigma_s C_e, \quad (\text{A4})$$

where the spontaneous distortion parameters Q_s and σ_s are evaluated at any temperature in the tetragonal phase (B_e and C_e are assumed to be temperature independent).¹ Equation (A2) now becomes

$$dT_c/d\tau_3 = \sigma_s [3\pi^2 M Q_s^2 (d\nu^2/dT)]^{-1}, \quad (\text{A5})$$

which relates only experimental quantities. The quan-

tity $d\nu^2/dT = 1.125 \times 10^{22} \text{ Hz}^2/\text{K}$ has been measured in the cubic phase, using inelastic scattering, by Cowley *et al.*³⁹ Substituting values taken from Sec. IV for the other parameters in (A5), we find $dT_c/d\tau_3 = 7.5 \times 10^{-3} \text{ K/at.}$, to be compared with the value $(18 \pm 2) \times 10^{-3}$ observed by Sorge *et al.*,¹¹ according to Pietrass and Hegenbarth.¹⁰ This discrepancy appears to be outside the bounds of experimental error. We note also that our (A5) above is equivalent to Eqs. (6) and (7) of Rehwald.²⁹

* Permanent address: IBM Thomas J. Watson Research Center, Yorktown Heights, N.Y. 10598.

¹ J. C. Slonczewski and H. Thomas, Phys. Rev. B **1**, 3599 (1970).

² A. Lauberau (unpublished).

³ J. Feder and E. Pytte, Phys. Rev. B **1**, 4803 (1970).

⁴ E. Pytte and J. Feder, Phys. Rev. **187**, 1077 (1969).

⁵ E. Pytte, Phys. Rev. B **1**, 924 (1970).

⁶ P. C. Kwok and P. B. Miller, Phys. Rev. **151**, 387 (1966), and references contained therein.

⁷ S. E. Stokowski and A. L. Schawlow, Phys. Rev. **178**, 457 (1969).

⁸ S. E. Stokowski and A. L. Schawlow, Phys. Rev. **178**, 464 (1969).

⁹ W. J. Burke and R. J. Pressley, Solid State Commun. **7**, 1187 (1969). {*Note added in proof.* The stress-induced transition has now been confirmed by means of EPR [K. A. Müller, W. Berlinger, and J. C. Slonczewski, Phys. Rev. Letters **25**, 734 (1970)] and optical spectroscopy [Ref. 17 below; T. S. Chang, J. F. Holzrichter, G. F. Imbusch, and A. L. Schawlow, Solid State Commun. **8**, 1179 (1970); L. S. Wall, M. Rokni, and A. L. Schawlow (unpublished)]. The results are consistent with our theory.}

¹⁰ B. Pietrass and E. Hegenbarth, Phys. Status Solidi **34**, K119 (1969).

¹¹ G. Sorge, G. Schmidt, E. Hegenbarth, and C. Frenzel, Phys. Status Solidi **37**, K17 (1970); and G. Sorge, G. Schmidt, and E. Hegenbarth (unpublished, quoted in Ref. 10).

¹² B. Alefeld, Z. Physik **222**, 155 (1969).

¹³ R. O. Bell and G. Rupprecht, Phys. Rev. **129**, 90 (1963).

¹⁴ P. A. Fleury, J. F. Scott, and J. M. Worlock, Phys. Rev. Letters **21**, 16 (1968).

¹⁵ G. Shirane and Y. Yamada, Phys. Rev. **177**, 858 (1969).

¹⁶ F. W. Lytle, J. Appl. Phys. **35**, 2212 (1964).

¹⁷ W. J. Burke, R. J. Pressley, and J. C. Slonczewski, Solid State Commun. (to be published).

¹⁸ K. A. Müller, W. Berlinger, and F. Waldner, Phys. Rev. Letters **21**, 814 (1968).

¹⁹ A. L. Schawlow, A. H. Piksiss, and S. Sugano, Phys. Rev. **122**, 1469 (1961).

²⁰ K. A. Müller, Arch. Sci. (Geneva) **11**, 150 (1958).

²¹ G. F. Koster, J. O. Dimmock, R. G. Wheeler, and H. Statz,

Properties of the Thirty-Two Point Groups (MIT, Cambridge, Mass., 1963).

²² Y. Tanabe and S. Sugano, J. Phys. Soc. Japan **9**, 753 (1954); **11**, 864 (1956).

²³ H. A. Jahn, Proc. Roy. Soc. (London) **A164**, 117 (1938).

²⁴ E. O. Kane, J. Phys. Chem. Solids **1**, 82 (1956).

²⁵ E. P. Wigner, *Group Theory* (Academic, New York, 1959).

²⁶ According to a private communication, B. Lüthi recently observed a value of \bar{V}_l which is smaller than that found in Ref. 13, but close to the value calculated in ST from Brillouin data. Adoption of the new value would tend to change our calculated \bar{p}_c in the direction of the experimental value. [See B. Lüthi and T. J. Moran, Phys. Rev. B **2**, 1211 (1970).]

²⁷ B. Derighetti, J. E. Drumheller, F. Laves, K. A. Müller, and F. Waldner, Acta Cryst. **18**, 557 (1965); C. de Rango, J. Tsoucaris, and C. Zelwer, *ibid.* **20**, 590 (1966).

²⁸ S. Geller and V. B. Bala, Acta Cryst. **9**, 1019 (1956).

²⁹ W. Rehwald (unpublished).

³⁰ This suggestion was made to the author by W. J. Burke in private discussions.

³¹ H. E. Weaver, J. Phys. Chem. Solids **11**, 274 (1959).

³² J. M. Worlock and P. A. Fleury, Phys. Rev. Letters **19**, 1176 (1967); P. A. Fleury and J. M. Worlock, Phys. Rev. **174**, 613 (1968).

³³ S. E. Stokowski and A. L. Schawlow, Phys. Rev. Letters **21**, 965 (1968).

³⁴ H. Unoki and T. Sakudo, International Conference on Ferroelectricity, Kyoto, 1969 (unpublished).

³⁵ J. H. Griffith, *The Theory of Transition-Metal Ions* (Cambridge U.P., London, 1961).

³⁶ See the review paper by F. Ham, in *Electron Paramagnetic Resonance*, edited by S. Geschwind (Plenum, New York, to be published).

³⁷ J. C. Slonczewski, K. A. Müller, and W. Berlinger, Phys. Rev. B **1**, 3545 (1970).

³⁸ Our \bar{p} is $-P$ in the notation of Ref. 19. However, the positive signs of the mean-shift coefficients reported in their Table I are obviously incorrect because the data plots show the mean shift decreasing with increasing stress magnitude.

³⁹ R. A. Cowley, W. G. L. Buyers, and G. Dolling, Solid State Commun. **7**, 181 (1969). Essentially the same results for $\nu(T)$ are reported in Ref. 15.